

A Dynamical Model for Nuclear Structure Functions

D. Indumathi,

Institut für Physik, Universität Dortmund, D 44221, Dortmund, Germany

Wei Zhu,

CCAST (World Laboratory) P.O. Box 8730, Beijing 100080, P. R. China

and

Dept. of Physics, East China Normal University, Shanghai 200062, P. R. China

Abstract

We construct a dynamical model for the parton distributions in a nucleus by perturbative evolution of input distributions from a low starting scale. These input distributions are obtained by modifications of the corresponding free nucleon ones; the modifications being determined by standard nuclear physics considerations. The model gives good agreement with existing data. Its extension to the spin dependent case enables an estimation of nuclear modifications to asymmetries observed in recent doubly polarised deep inelastic scattering experiments. Although the structure functions themselves are very different from the free nucleon ones, their ratio is insensitive to these changes.

1 Introduction

The fact that the structure functions of bound and free nucleons are not equal is called the EMC effect [1]. Although this discovery was made nearly fifteen years ago, the origin of the EMC effect is still an open problem [2, 3, 4]. Recently, accurate data on the structure function ratios, $F_2^A(x, Q^2)/F_2^N(x, Q^2)$, has been obtained by various groups [5, 6, 7] on a host of nuclei with mass numbers ranging from $A = 4$ (Helium) to $A = 118$ (Tin). Combining these measurements with new data on the free proton and deuteron structure functions, $F_2^p(x, Q^2)$ and $F_2^N(x, Q^2)$, which are measured down to small x values at HERA and NMC

[8, 9], we have the nuclear structure function (per nucleon), $F_2^A(x, Q^2)$. The free nucleon data thus set a more stringent demand on the theory of the EMC effect: the model should explain not only the ratios of the structure functions but the absolute values of the nuclear structure functions themselves.

In this paper, we propose an extension of the dynamical model of the proton structure function due to Glück, Reya, and Vogt (GRV) [10], to the nuclear case. This model successfully fits existing free proton data down to very small $Q^2 \simeq 0.5\text{--}1 \text{ GeV}^2$. It uses an input set of parton distributions at a low starting scale, $Q^2 = \mu^2$, which are dynamically evolved using the DGLAP equations [11] to obtain the distributions and hence the structure functions at larger values of Q^2 . In our extension of this model to the case of nuclear parton distributions, the free nucleon input is modified due to nuclear effects; these are then evolved using the same DGLAP equations in order to obtain the corresponding nuclear parton densities at larger Q^2 . We also apply the model to the case of spin dependent density distributions.

The main ingredients of our model (common to both the spin independent as well as the spin dependent case) are as follows: At a low starting scale, $Q^2 = \mu^2$, we picture the nucleon (either free or bound) as being composed of valence quarks, gluons, and a mesonic sea. However, all the parton densities in a bound nucleon are different from those in a free one. This is because of swelling of a bound nucleon, which causes a modification of the partonic distributions. With the exception of one free parameter (which characterises the extent of swelling), the bound-nucleon parton distributions are exactly computable in terms of the known free-nucleon ones. Nuclear binding effects then cause a further depletion of the meson component of a bound nucleon. The extent of depletion is fixed using standard inputs from nuclear physics. Both swelling and binding have been applied before to the same problem [4, 12, 13]; however, we implement these effects in our model *in a totally different manner*. These two effects therefore completely specify our input bound-nucleon distributions at $Q^2 = \mu^2$. These are then evolved as usual using the DGLAP equations to give the nuclear density distributions at any desired value of (x, Q^2) . A further depletion of the small- x densities occurs at the time of interaction. This is because parton overlap can occur with the nuclear medium, resulting in a further modification of the structure function at the scale determined by the interaction, viz., at Q^2 . This is similar in nature to the binding effect, and will be discussed in more detail in what follows.

The prescription for modification of the parton densities in a free nucleon in terms of

nuclear effects can be straightforwardly extended to the case of *spin dependent* parton densities. It is interesting to study this as data on the spin dependent deuteron and neutron structure functions have been obtained [14] from deuteron and ^3He targets. The data have typically been analysed assuming that nuclear effects are small in such measurements, and can thus be ignored. Our main conclusion [15] is that the individual (spin independent as well as spin dependent) structure functions undergo substantial modifications due to nuclear effects; however, their *ratio*—the asymmetry—which is the measured quantity, is largely free from these and so gives hope that the neutron structure function may be unambiguously determined from such a measurement.

We find that our model explains all the available data over almost the entire kinematic range in (x, Q^2) . We now discuss each of these effects in more detail. In Section 2, we outline the original GRV approach to determining the free nucleon structure functions, since this is the basis upon which our model is constructed. In Section 3, we work out the bound-nucleon spin independent structure functions, and demonstrate the agreement of the model predictions with the data. In Section 4, we work out the spin dependent case and indicate how it influences the extraction of the spin dependent structure function; a major portion of the results contained in this section has already appeared elsewhere [15]. Section 5 contains some remarks on the individual parton distributions, especially the valence distributions, while Section 6 concludes the paper.

2 The Parton Distributions in a Free Nucleon

We work at a low starting scale of $Q^2 = \mu^2 \simeq 0.23 \text{ GeV}^2$. At this low scale—the closest to the confinement scale at which a perturbative description of the nucleonic parton content is still meaningful [10]—the nucleon is composed of valence quarks, gluons and a mesonic sea. Defining q_f^+ and q_f^- to be the positive and negative helicity densities of f -flavour quarks in either free or bound nucleons, we can define the following spin independent and spin dependent combinations respectively:

$$\begin{aligned} q_f(x) &= q_f^+(x) + q_f^-(x) ; \\ \tilde{q}_f(x) &= q_f^+(x) - q_f^-(x) . \end{aligned} \tag{1}$$

A similar definition holds for the gluons as well. Given suitable parametrisations of these densities at this scale (the so-called “input densities”), the Altarelli Parisi (DGLAP) equations

[11] can be used to perturbatively evolve the densities to any larger scale, Q^2 , of interest, where they can be compared with the data. Such a parametrisation for the spin independent densities in the free-nucleon case exists, is due to Glück, Reya, and Vogt [10] (GRV), and exhibits very good agreement with data amassed from various sources over a very large kinematical region, and certainly in that of the EMC effect, where Q^2 ranges from less than 1 GeV² to around a 100 GeV². We thus propose to use this parametrisation as a starting point in our corresponding unpolarised model for bound-nucleon parton distributions.

In principle, it is possible to use other available parametrisations [16, 17]. However, we find the GRV most appropriate for our purpose as each of their input densities is integrable (there are finite number of partons at μ^2). Every parton distribution is generated dynamically by evolution from a set of valence-like inputs of the form

$$xq_N(x, \mu^2) = Nx^\alpha(1-x)^\beta P_{N,q}(x) ; \alpha > 0 , \quad (2)$$

at μ^2 . For example, in the leading order (LO) approximation with $\mu^2 = 0.23 \text{ GeV}^2$, the valence (u_v, d_v), the total sea (S), and gluon (g) input distributions in a free proton are given to be [10],

$$\begin{aligned} xu_v^N(x, \mu^2) &= 1.377x^{0.549}(x)(1-x)^{3.027} P_{N,u} , \\ xd_v^N(x, \mu^2) &= 0.328x^{0.366}(x)(1-x)^{3.744} P_{N,d} , \\ xS_N(x, \mu^2) &= 2x(\bar{u} + \bar{d}) = 2.40x^{0.29}(x)(1-x)^{7.88} P_{N,S} , \\ xg_N(x, \mu^2) &= 35.8x^{2.3}(1-x)^{4.0} , \end{aligned} \quad (3a)$$

where the polynomials, $P_{N,q}$, with the subscript N referring to a free proton, are,

$$\begin{aligned} P_{N,u} &= 1 + 0.81\sqrt{x} - 4.36x + 19.4x^{3/2} , \\ P_{N,d} &= 1 + 1.14\sqrt{x} + 5.71x + 16.9x^{3/2} , \\ P_{N,S} &= 1 + 0.31x . \end{aligned} \quad (3b)$$

The corresponding neutron densities can be obtained from isospin symmetry, and hence the deuteron distributions as well, by averaging the two. These densities, q_N, g , are valence-like in the sense that they are integrable at this scale; this will prove an important consideration when we extend this model to the nuclear case. At this low scale, we have the following physical interpretation of the free-nucleon distribution: the valence quarks and gluons are co-moving and constitute the pure nucleonic component of the proton, while the sea quarks comprise the mesonic component of the proton. This idea is reinforced by the observation

that the sea quark distribution is much softer than that of the valence quarks or gluons (compare the exponent β for the sea densities with that for the valence or gluon densities), which could possibly arise from a convolution model for mesons in nucleons [18]. Such a picture remains valid in the bound-nucleon case and will be applied when describing nuclear modifications due to binding.

The Q^2 evolution of these densities to leading order are given in terms of the well-known splitting functions calculable from QCD; using these, and the DGLAP equations [11], the densities $q_N(x, Q^2)$, at any $Q^2 > \mu^2$ can be determined. These, as we have remarked before, show good agreement with available data.

The Glück, Reya, and Vogelsang (GRVs) [19] parametrisation contains the analogous treatment of the spin dependent densities, $\tilde{q}_N(x, \mu^2)$, which are used as an input in the corresponding polarised problem. These densities are also parametrised in a form similar to eq (2), and at the same value of μ^2 (this is necessary in order to retain the definition (1)); in fact, every spin dependent density is a factor of the form of the RHS of (2) times the corresponding unpolarised density as given by the GRV set. Hence the number of partons (of either helicity) is still finite. Specifically, the spin dependent inputs for the LO valence (\tilde{u}_V , \tilde{d}_V), sea (\tilde{S} for the total nonstrange sea, and \tilde{s} for the strange sea) and gluon (\tilde{g}) densities in the GRVs standard scenario [19] are given by,

$$\begin{aligned}
\tilde{u}_V(x, \mu^2) &= 0.718x^{0.2}u_V(x, \mu^2) , \\
\tilde{d}_V(x, \mu^2) &= -0.728x^{0.39}d_V(x, \mu^2) , \\
\tilde{S}(x, \mu^2) &= -2.018x(1-x)^{0.3}S(x, \mu^2) , \\
\tilde{s}(x, \mu^2) &= 0.36S(x, \mu^2) , \\
\tilde{g}(x, \mu^2) &= 16.55x(1-x)^{5.82}g(x, \mu^2) .
\end{aligned}
\tag{4}$$

Our aim then is to compute nuclear effects and the consequent modification of these free-nucleon input parton distributions in a nucleon bound in a(n isoscalar) nucleus of mass A . We begin with nuclear modifications in the case of spin independent lepton nucleus deep inelastic scattering.

3 The Model: Spin Independent Case

In order to retain compatibility with the free nucleon case, we work at the same input scale of $Q^2 = \mu^2 = 0.23 \text{ GeV}^2$. In other words, we begin with the input distributions described

by (3) and compute modifications of every parton distribution due to nuclear swelling and binding. We then evolve the resulting *nuclear* input distributions to the scale Q^2 , and include the effects due to parton–nucleon overlap to obtain the nuclear spin independent structure functions at that scale. We now describe the swelling effect at the input scale μ^2 .

3.1 The Swelling Effect

Swelling was first discussed by Jaffe [12] in the context of 6–quark bags within the bound nucleon. The presence of such structures within the bound nucleon could substantially increase the confinement radius. This confinement scale change (in which the input point, μ^2 , is rescaled), was then re-expressed in terms of a change of the scale variable, $Q^2 \rightarrow \xi Q^2$; these rescaling models were then able to explain the EMC effect, especially in the medium x region [13, 20].

Here, we interpret swelling as an increase in the *physical* size of a bound nucleon. This swelling only geometrically redistributes partons inside the nucleon and does not change either the value of the dynamical parameter, μ , or the existing number of partons at μ^2 . Such an interpretation and description of the swelling effect using some universal principles was first discussed in a valon model by Zhu and Shen [21]. The relative increase in the nucleon’s radius is δ_A , where $(R_N + \Delta R(A))/R_N = 1 + \delta_A$. While δ_A is not known, its A -dependence can be written down:

$$\delta_A = [1 - P_s(A)]\delta_{\text{vol}} + P_s(A)\delta_{\text{vol}}/2 . \quad (5)$$

The second term corrects for the fact that the swelling of a nucleon on the nuclear surface is less than that of one in the interior. $P_s(A)$ is the probability of finding a nucleon on the nuclear surface; it is known, and its value is discussed below. Here δ_{vol} parametrises the swelling of the nucleon in the interior of a heavy nucleus and is the only free parameter in our work. It is a constant for nuclei with $A > 12$ and also for Helium (with $P_s = 1$) since they have similar nuclear densities. We emphasise that the distortions of the density distributions, being purely geometrical, conserve the total parton number and momentum of each parton species (i.e., the first and second moments of the distributions are unchanged). Furthermore, the third moments are modified in a well-determined way.

Specifically, the first three moments of the parton distributions in a free (q_N) and bound

(q_A) nucleon at μ^2 are related by

$$\begin{aligned} \langle q_A(\mu^2) \rangle_1 &= \langle q_N(\mu^2) \rangle_1 , \\ \langle q_A(\mu^2) \rangle_2 &= \langle q_N(\mu^2) \rangle_2 , \\ \frac{(\langle q_N(\mu^2) \rangle_3 - \langle q_N(\mu^2) \rangle_2^2)^{1/2}}{(\langle q_A(\mu^2) \rangle_3 - \langle q_A(\mu^2) \rangle_2^2)^{1/2}} &= 1 + \delta_A . \end{aligned} \tag{6}$$

The first two equations imply number and momentum conservation of each parton type in free and bound nuclei. The last incorporates the effect of a size increase of the bound nucleon: according to Heisenberg’s uncertainty principle, this results in a pinching of the momentum distribution, making the bound density distribution narrower and sharper than the free nucleon ones [21]. This causes not only a depletion of *all* parton densities at large- and small- x , but also an enhancement at intermediate- x .

It is clear that we can use these as constraint equations to determine the bound-nucleon densities q_A (for q = valence quarks, sea quarks, and gluons) in terms of the free densities, q_N , using (3) and (6). We take $P_{A,q}(x) = P_{N,q}(x)$, for simplicity. Then the changes in the three main parameters, N , α , and β , in (2), due to swelling, are immediately determined by the three constraints in (6). Thus the input bound-nucleon densities at $Q^2 = \mu^2$ are now fixed applying the energy–momentum constraint and the Uncertainty principle, and using the corresponding free–nucleon densities. Fig. 1 gives an example of the swelling effect for the parton densities in calcium. The momenta lost from the small and large x regions are transferred to the intermediate x region. The effect thus not only modifies the structure function itself, but also weakly enhances the distributions in the region $0.1 < x < 0.3$ and results in “antishadowing”. This enhancement depends on the nuclear density (through δ_A) and, furthermore, does not disappear at larger Q^2 for the case of the valence densities. We will comment on this further in Section 5.

These modified input densities are then further modified due to the effect of nuclear binding, which we now discuss.

3.2 The Binding Effect

The bound nucleon is in an attractive potential, V ; $V < 0$. In traditional binding models [4, 22], the effective mass of the nucleon is taken as

$$M_{N,\text{eff}}^{\text{trad}} = M_N + V + T \simeq M_N + \varepsilon , \tag{7}$$

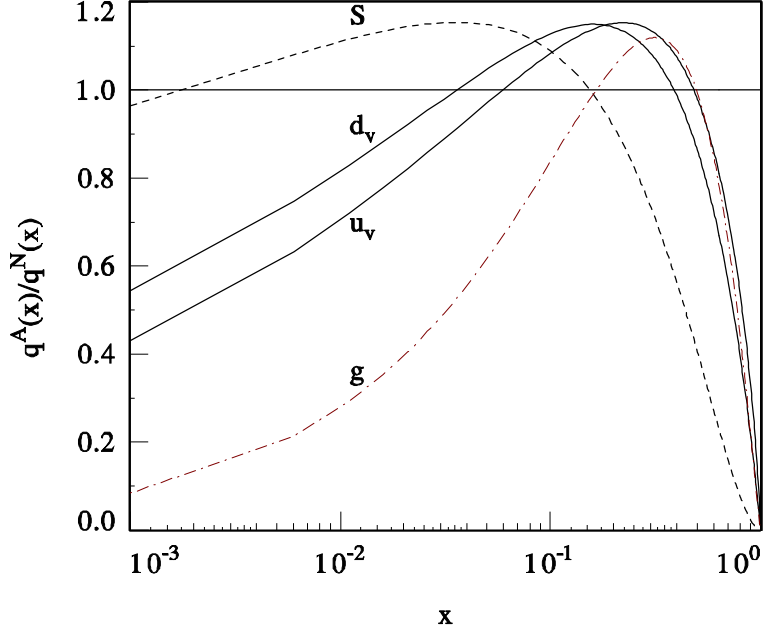


Figure 1: The effect of nucleon swelling on the calcium input distributions: the ratios of the modified to unmodified densities are shown for u_v , d_v , S , and g .

where $\varepsilon \simeq V + T$ is the average separation (or removal) energy and the mean kinetic energy is $T = \langle p^2 \rangle / 2M_N = 3p_F^2 / 10M_N$ with p_F the Fermi momentum. The average binding energy per nucleon is,

$$b = -(\varepsilon + T)/2 . \quad (8)$$

The factor 2 in (8) is due to the fact that, within the approximation of two-body scattering, the nucleus with mass $(A - 1)$ that is formed after the interaction is required to be on mass-shell.

A consequence of (7) is a shift in the scaling variable from $x = Q^2 / (2M_N\nu)$ towards $x' = x / \langle z \rangle$ with $\langle z \rangle = 1 + \varepsilon / M_N$. This x -rescaling obviously reduces the momentum of the valence quarks and explains the traditional EMC effect (in the intermediate x region). Excess mesons with energy $E_\pi \approx T$ are therefore introduced to compensate this energy-momentum loss. Hence the energy of the additional mesonic fields comes mainly from the valence quarks. Unfortunately, these kind of binding models met with difficulty since the FNAL experiment [23] excluded a net enhancement of mesonic fields in the nucleus.

In our model, we consider that the attractive potential describing the nuclear force arises from the exchange of mesons. At the starting scale, $Q^2 = \mu^2$, the bound nucleon is made

up of valence quarks, gluons and mesons; hence, a reasonable assumption is that the nuclear binding effect reduces only the mesonic fields of the nucleon at this scale. Furthermore, we regard the enhanced mesonic fields, which are a consequence of binding, as a part of the individual nucleon itself, since the probe cannot distinguish between the distributions of the original mesonic fields and that of the compensative mesonic fields. The effective mass of the bound nucleon is then

$$M_{N,\text{eff}} = M_N + V + T + E_\pi = M_N - 2b. \quad (9)$$

Hence binding causes a loss of energy from the nucleons in a nucleus; the total energy-momentum of the nucleus (which is conserved) is obtained on adding the contribution from the total binding energy to that of the nucleons. Fermi motion further smears the parton distributions, but near $x = 1 - 2b/M_N$. Since we are interested here primarily in the small and intermediate x region, we do not consider this effect in what follows.

The expression (9) allows us to simply establish the connection between the binding effect and parton distributions in nuclei using the Weizsäcker mass formula [24]. According to this formula, the binding energy per nucleon arising strictly from the nuclear force is

$$b = [1 - P_s(A)]a_{\text{vol}} + P_s(A)\frac{a_{\text{vol}}}{2} = a_{\text{vol}} - a_{\text{sur}}A^{-1/3}, \quad (10)$$

for $A > 12$, where $P_s(A)$ is the probability of finding a nucleon on the nuclear surface. Experimentally $a_{\text{vol}} = 15.67$ MeV, and $a_{\text{sur}} = 17.23$ MeV.

Coulombic interactions among nucleons will change the partonic photon distributions and indirectly increase both the effective mass of the charged partons, $m_{\text{eff}} \rightarrow m'_{\text{eff}}$ and that of the nucleon, $M_{N,\text{eff}} \rightarrow M'_{N,\text{eff}}$. Since the charged partons carry most of the nucleon momentum at $Q^2 = \mu^2$, the scaling variable $x' \simeq m'_{\text{eff}}/M'_{N,\text{eff}} \simeq m_{\text{eff}}/M_{N,\text{eff}} \simeq x$. Therefore, we ignore the contributions of the Coulombic term in the mass formula.

The binding energy, b , corresponds to loss of energy of the “mesonic” component of the nucleons in our model. This means that the momentum fraction carried by the mesons in a nucleon bound in a nucleus at $Q^2 = \mu^2$ will be reduced from the free-nucleon density. Since we have identified these to be the sea quarks in our model, the bound nucleon sea density is reduced from the free nucleon one, $S_N(x, \mu^2)$, to

$$\begin{aligned} S_A(x, \mu^2) &= K(A)S_N(x, \mu^2) \\ &= \left(1 - \frac{2b}{M_N \langle S_N(\mu^2) \rangle_2}\right) S_N(x, \mu^2). \end{aligned} \quad (11)$$

Here $\langle S_N \rangle_2$ is the momentum fraction (second moment) of the mesons and the decrease in number of mesons due to the binding effect is simply made proportional to the quark density. Since the mesons are soft, this is a small- x effect. The binding effect is weaker in our model since $2b \ll -\varepsilon$; the observed depletion of the nuclear structure function at larger x values (the traditional EMC effect) comes from elsewhere; in fact, it comes from modification of the densities due to swelling.

Hence, swelling prescribes the bound-nucleon densities at the input scale, μ^2 . The sea densities are additionally depleted due to binding effects. These distributions can now be evolved to any scale, $Q^2 > \mu^2$, using the DGLAP equations. Before we use these to compute the structure functions at this scale, however, we must incorporate one more phenomenon.

3.3 The Second Binding Effect

There is a further depletion of the sea densities which occurs at the time of scattering, due to nucleon nucleon interaction, arising from parton–nucleon overlap. Similar to (11), this causes a loss in number of sea quarks which is proportional to the original density, i.e.,

$$S_A(x, Q^2) - S'_A(x, Q^2) \propto S_A(x, Q^2) .$$

The physical origin of this depletion is easiest to see in the Breit frame, where the exchanged virtual boson is completely space-like, so that the 3–momentum of the struck parton is flipped in the interaction. Hence, due to the uncertainty principle, a struck parton carrying a fraction x of the nucleon’s momentum, P_N , during the interaction time $\tau_{\text{int}} = 1/\nu$, will be off shell and localized longitudinally to within a potentially large distance $\Delta Z \sim 1/(2xP_N)$, which may exceed the average 2–nucleon separation for a small enough $x < x_0$, where x_0 is defined below.

Binding usually occurs due to overlap of wave functions of neighbouring nucleons. In a static nucleus, it is therefore sufficient to consider just the binding between a nucleon and all its neighbours, and so define an average binding energy per nucleon based on nearest neighbour interactions. The effect of the Q^2 momentum transfer into the nucleus in deep inelastic scattering is to permit overlap of wave functions between two nucleons which are not otherwise in contact. We parametrise this by the simple ansatz that every overlap of the parton with a nucleon causes energy loss, similar to binding. Hence we call this the second binding effect. The energy loss due to this effect is from sea quarks and gluons. (Valence

quarks are not depleted due to the requirement of quantum number conservation). The energy loss due to this effect from sea quarks in a bound nucleon due to interaction with one other nucleon is therefore,

$$U_s(Q^2) = \beta M_N \int_0^{x_0} x S_A(x, Q^2) \simeq \beta M_N \langle S_A(Q^2) \rangle_2 ,$$

and we assume that the strength of this interaction is the same as that due to binding, viz.,

$$\beta = \frac{U_s(Q^2)}{M_N \langle S_A(Q^2) \rangle_2} = \frac{U(\mu^2)}{M_N \langle S_N(\mu^2) \rangle_2} , \quad (12)$$

$U(\mu^2) = a_{\text{vol}}/6$ being the binding energy between each pair of nucleons. Here, we have ignored the possible Q^2 dependence of β . The only rôle of Q^2 here is to provide the impulse which allows the parton–nucleon overlap to occur.

The shadowing begins at $x = x_0 = 1/(2M_N d_N)$. Here d_N is the average correlation distance between two neighbouring nucleons in the lab frame:

$$d_N = P_s(A) [R_N + (D_S - 2R_N)] + (1 - P_s(A)) \left[\frac{R_N}{2} + (D_S - 2R_N) \right] , \quad (13)$$

where R_N is the nucleon radius and D_S is the average 2–nucleon separation, and we have corrected for surface effects in the usual manner. The shadowing effect saturates when the struck quark wave function completely overlaps the nucleus in the z -direction, at $x = x_A$. A parton with an intermediate momentum fraction, x , can overlap $(n - 1)$ other nucleons, where $n = 1/(2M_N d_N x) = x_0/x$. Due to the applicability of the superposition principle, the loss of energy due to interaction with each of the nucleons over which the struck quark wave function extends, is equal and additive. The total shadowing of the sea quarks is thus given by

$$S'_A(x, Q^2) = K'(A) S_A(x, Q^2) ,$$

where the depletion factor is,

$$\begin{aligned} K'(A) &= 1, & \text{when } x > x_0; \\ &= 1 - 2\beta(x_0 x^{-1} - 1), & \text{when } x_A < x < x_0; \\ &= 1 - 2\beta(x_0 x_A^{-1} - 1), & \text{when } x < x_A, \end{aligned} \quad (14)$$

where $2\beta = 0.037$, $x_A = 1/(4\bar{R}_A M_N)$, and $2\bar{R}_A \simeq 1.4R_A$ is the average thickness of the nucleus. Since $x_0 \lesssim 0.1$, this is a small x effect. We emphasize that this effect, caused by parton–nucleon overlap, acts on the intermediate state of the probe–target interaction and

does not participate in the QCD evolution of the initial state. Hence it cannot “disappear” on evolution of the input parton densities from the input scale. However, as $Q^2 \rightarrow \infty$, $\tau_{int} \rightarrow 0$; the overlap time (time for interaction due to parton-nucleon overlap) goes to zero, and hence such a nucleon–nucleon interaction cannot occur. The model is therefore best applied to (maybe large, but) finite Q^2 . We are now ready to write down the bound-nucleon structure function and effect a comparison with data.

3.4 The Structure Function, $F_2^A(x, Q^2)$

The input nucleon structure function (for an isoscalar nucleus) is given by

$$F_2^A(x, \mu^2) = \langle e^2 \rangle \left[xu_v^A(x, \mu^2) + xd_v^A(x, \mu^2) + K(A)xS_A(x, \mu^2) \right], \quad (15)$$

where the average charge square factor is $\langle e^2 \rangle = 5/18$; $q^A(x, \mu^2)$ incorporates the effect of swelling on every input parton density, $q^N(x, \mu^2)$, and $K(A)$ incorporates the binding effect. At a larger scale Q^2 , the second binding effect also plays a rôle in modifying the sea densities. The structure function ratio of nucleons bound in two different nuclei, A and B , at $Q^2 > \mu^2$ is thus given by,

$$R^{AB} = \frac{xu_v^A(x, Q^2) + xd_v^A(x, Q^2) + K'(A)x\hat{S}_A(x, Q^2)}{xu_v^B(x, Q^2) + xd_v^B(x, Q^2) + K'(B)x\hat{S}_B(x, Q^2)}, \quad (16)$$

where $\hat{S}_A(x, Q^2)$ corresponds to the (leading order) evolution [11] of $K(A)S_A(x, \mu^2)$, i.e., of the swelled input sea density, depleted by the binding effect, to the scale Q^2 , and $K'(A)$ incorporates the second binding effect at the scale Q^2 . Note that for $Q^2 > \mu^2$, the sea density also includes a finite contribution from strange quarks. The smearing effect of Fermi motion (at large x) is neglected in this work for simplicity. Hence our results are not valid at large x . Including this effect by means of the usual convolution formula [12] will give the typical depletion and then rise of R as $x \rightarrow 1$, but will not affect our small- and intermediate- x results.

In fig. 2 we give our predictions for the x , Q^2 , and A dependences of the ratios for He/D, C/D and Ca/D. The only free parameter to be fixed in computing these ratios is the value of δ_{vol} that parametrises the swelling. We find that $\delta_{vol} = 0.15$ best describes the various available data for these nuclei.

We have also shown the ratio of the ${}^6\text{Li}$ to D structure functions in fig. 2. Unlike helium (which also has $A < 12$), lithium is a very loosely bound nucleus (whose density is less than

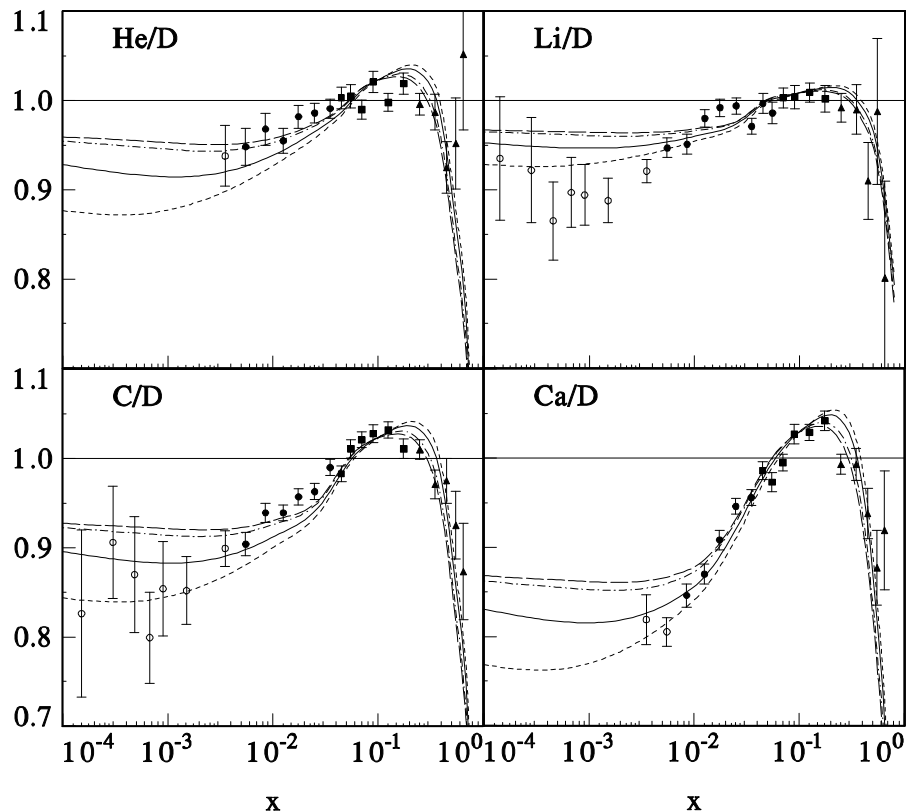


Figure 2: The structure function ratios as functions of x for (a) He/D, (b) Li/D, (c) C/D, and (d) Ca/D. The dashed, full, broken, and long-dashed curves correspond to $Q^2 = 0.5, 1, 5,$ and 15 GeV^2 respectively. The data [6, 7], shown as open and solid circles, boxes and triangles correspond to $Q^2 < 1, 1-5, 5-15,$ and $> 15 \text{ GeV}^2$ respectively.

half that of helium or carbon, while its radius is larger than that of carbon [5]). Hence, δ_A for Li can be expected to be much smaller than that for He ($\delta_{\text{He}} = 0.15/2$ according to (5)) and we take it to be 0.033. In all cases, the swelling effect dominates the intermediate x ratios while both the binding effects determine the small x ratios.

The ratios $R^{\text{AB}} = F_2^{\text{A}}/F_2^{\text{B}}$ for A/B corresponding to C/Li, Ca/Li, and Ca/C are more sensitively dependent on the model of the EMC effect (as seen in fig. 3). We predict, in general, an enhancement of the ratio, R^{AB} , at intermediate x which is a net effect of the swelling and the first binding effect, both of which depend on the nuclear density. On the other hand, the strong depletion at small x depends on both the nuclear radius and density. The weaker enhancement of the intermediate x ratios of Ca and C is because of their similar densities [25] as compared to the C/Li and Ca/Li ratios where the two nuclei have different densities. Our predictions are seen to be in excellent agreement with the NMC data [6], also

shown for the sake of comparison.

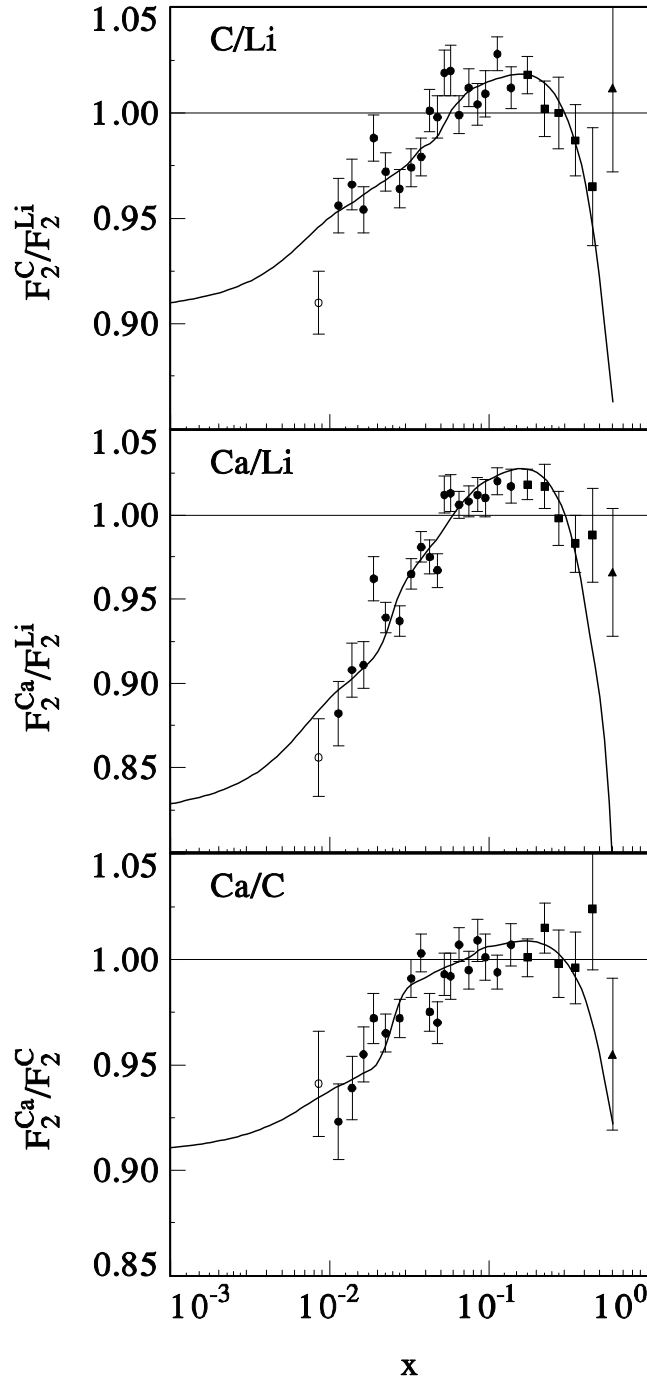


Figure 3: The structure function ratios for (a) C/Li, (b) Ca/Li, and (c) Ca/C. The solid curve is a smooth fit to our theoretical predictions at the same (x, Q^2) as each available data point [6], with $Q^2 = 0.5 \text{ GeV}^2$ when extrapolating to small x . The description of the data is the same as in fig. 2.

Note that we have computed these three ratios at the *same* values of (x, Q^2) as the data.

Finally, the NMC has recently obtained data on the structure function ratio in Tin to Carbon [26]. The (preliminary) data and our model predictions, again at the same (x, Q^2) as the data, are plotted in fig. 4. We see that there is again good agreement with the data in the region of validity of our model ($x < 0.6$). We emphasize that, apart from the swelling parameter, δ_{vol} , all parameters are fixed by a few fundamental nuclear inputs.

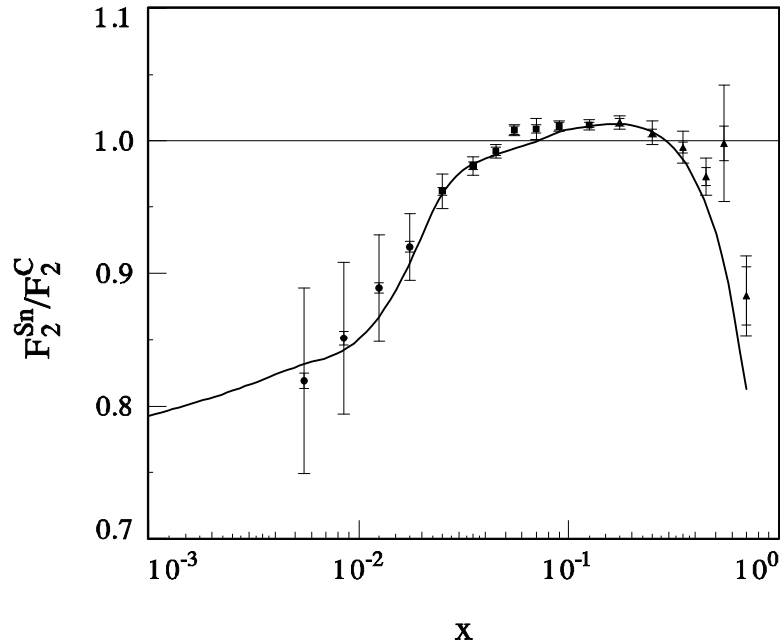


Figure 4: The structure function ratio for Sn/C. The solid curve is a smooth fit to our theoretical predictions at the same (x, Q^2) as each available data point [26], with $Q^2 = 0.5 \text{ GeV}^2$ when extrapolating to small x . The description of the data is the same as in fig. 2, with both statistical as well as total (statistical and systematic, added in quadrature) errors shown.

The input (3) reliably predicts the free nucleon structure function in the region $Q^2 \gtrsim 0.5 \text{ GeV}^2$. Hence our model is also expected to predict correctly, not only the ratios, but also the values of the nuclear structure functions themselves in the same kinematical region.

We now proceed to an analysis of the corresponding spin dependent densities.

4 The Model: Spin Dependent Case

As stated earlier, data on polarised neutron structure functions have been obtained using deuteron and helium targets [14]. Nuclear effects in deuteron are known to be small (though

measurable), since the deuteron is a loosely bound nucleus. There have been a number of papers [27] dealing with nuclear modifications of spin asymmetries and structure functions in the case of the deuteron¹. We therefore confine our attention to possible nuclear effects on the double spin asymmetry measurements made with helium nuclei. Woloshyn [28] showed that here the protonic contribution to the asymmetry is negligible so that the ³He double spin asymmetry is sensitive to the spin dependent neutron structure function, $g_1^n(x, Q^2)$, alone. However, there may be additional modifications of the spin dependent neutron structure function itself due to nuclear effects, as has been studied in various papers [15, 29]. These are especially of importance for checking the validity of the Bjorken Sum rule [30] that relates the difference of the first moments of the p and n spin dependent structure functions to the axial vector constant in nucleon beta decay. We therefore study nuclear effects on the spin dependent structure functions in our model.

The quantity of interest that is measured in polarised deep inelastic scattering measurements is the double spin asymmetry,

$$\mathcal{A}^A(x, Q^2) = \frac{g_1^A(x, Q^2)}{F_1^A(x, Q^2)}, \quad (17)$$

where g_1 and F_1 are the spin dependent and spin independent structure functions corresponding to the nucleus A . (We ignore the other structure function, g_2 , here). We are therefore interested in studying possible deviations, due to nuclear effects, of the measured asymmetry, \mathcal{A}^{He} , from the neutron asymmetry, \mathcal{A}^n , that is required to be extracted from the helium data.

Recall that the study of unpolarised bound nucleon densities used the GRV [10] density parametrisation as an input. We therefore use the corresponding GRVs [19] spin dependent densities as an input in the corresponding polarised problem. We proceed exactly as in the spin independent case.

4.1 The Input Spin Dependent Nuclear Distributions

The same nuclear effects of binding and swelling affect the spin dependent densities also. This is because they influence the positive and negative helicity densities, out of which the spin independent and spin dependent densities are composed (see eq (1)). The entire swelling

¹Depending on the model, corrections due to nuclear effects in deuterium can be as large as 10%.

effect can now be rephrased as the effect of swelling on individual *helicity* densities, so that equations analogous to (6) are valid for the spin dependent densities, $\tilde{q}(x)$, as well. This can be seen as follows: Swelling simply rearranges the parton distributions in the bound nucleon; there is no change in the number of each parton species. In particular, each helicity type is also conserved, i.e.,

$$\int q_A^+(x, \mu^2) dx = \int q_N^+(x, \mu^2) dx , \quad \int q_A^-(x, \mu^2) dx = \int q_N^-(x, \mu^2) dx .$$

Hence, their sum and difference is also conserved. The former (the spin independent combination) is contained in the first equation of the equation set (6); the latter implies, for the polarised combination,

$$\langle \widetilde{q}_A(\mu^2) \rangle_1 = \langle \widetilde{q}_N(\mu^2) \rangle_1 . \quad (18a)$$

(Note that $\langle q(\mu^2) \rangle_n = \langle q^+(\mu^2) \rangle_n + \langle q^-(\mu^2) \rangle_n$ for every moment, n , for both the free and bound nucleon, and similarly for the spin dependent combination as well). Similarly, since the momentum carried by each helicity density is unchanged, momentum conservation between the free and bound nucleon also holds for the sum and difference of the helicity densities. The corresponding equation for the sum is the second equation in (6); the equation for the helicity difference is

$$\langle \widetilde{q}_A(\mu^2) \rangle_2 = \langle \widetilde{q}_N(\mu^2) \rangle_2 . \quad (18b)$$

The extension of the third of the equations in (6) to the spin dependent case is not as straightforward. Every helicity density, $q_f^h(x)$, ($h = +, -$), spreads out over a larger size, or, equivalently, gets pinched in momentum space, according to Heisenberg's uncertainty relation, $\Delta p \Delta x = 1$. Applying this to each helicity type, for each flavour, we have,

$$\frac{(\langle q_N^+(\mu^2) \rangle_3 - \langle q_N^+(\mu^2) \rangle_2^2)^{1/2}}{(\langle q_A^+(\mu^2) \rangle_3 - \langle q_A^+(\mu^2) \rangle_2^2)^{1/2}} = 1 + \delta_A ; \quad \frac{(\langle q_N^-(\mu^2) \rangle_3 - \langle q_N^-(\mu^2) \rangle_2^2)^{1/2}}{(\langle q_A^-(\mu^2) \rangle_3 - \langle q_A^-(\mu^2) \rangle_2^2)^{1/2}} = 1 + \delta_A . \quad (19)$$

However, for later convenience, we prefer to use analogous expressions for the sum and difference, q_f and \tilde{q}_f , rather than for the individual helicity densities. Hence, the third of the constraints arising from swelling, i.e., the third of eq (6) and its spin dependent counterpart read,

$$\frac{(\langle q_N(\mu^2) \rangle_3 - \langle q_N(\mu^2) \rangle_2^2)^{1/2}}{(\langle q_A(\mu^2) \rangle_3 - \langle q_A(\mu^2) \rangle_2^2)^{1/2}} = 1 + \delta_A ; \quad \frac{(\langle \widetilde{q}_N(\mu^2) \rangle_3 - \langle \widetilde{q}_N(\mu^2) \rangle_2^2)^{1/2}}{(\langle \widetilde{q}_A(\mu^2) \rangle_3 - \langle \widetilde{q}_A(\mu^2) \rangle_2^2)^{1/2}} = 1 + \delta_A . \quad (18c)$$

The error involved between the exact expressions, eq (19), and their approximations, eq (18c), is a term proportional to $(1 - (1 + \delta_A)^2)$ and is of order δ_A . In principle, it is possible

to retain this term and compute the effects of swelling in both the spin independent and spin dependent sectors. However, this term mixes spin dependent and spin independent moments and thus implies that spin dependent moments affect spin independent bound-nucleon densities and vice versa, which is certainly unappealing; alternatively, since δ_A is small (about 10%), these error terms are small, and can be ignored. We prefer to take the latter approach. We are therefore justified in using eq (18c) rather than eq (19) to constrain the second moments of the parton densities. The three sets of equations, (18a–c), thus provide the three sets of constraint equations, analogous to the set (6), with which we can fix the input bound-nucleon spin dependent densities.

The modified input densities are thus determined, given a set of valid input free nucleon distributions, which we take to be the Glück, Reya, and Vogelsang 'standard' set (GRVs) [19] (see eq (4)). Once again, there are three constraint equations which serve to fix the three main parameters, α , β , and N for the corresponding bound-nucleon spin dependent densities. Note that δ_A is the same for the unpolarised as well as the polarised case. The effect of swelling on the spin dependent densities is thus similar to that on the spin independent ones, causing a narrowing of the density distributions, with resulting anti-shadowing in the intermediate- x region.

Binding causes loss of energy in the sea: this is due to loss of mesons from the nucleon. Since these mesons are spin-0 bosons, it is clear that no spin is lost from the sea due to binding (equal numbers of positive and negative helicity partners are lost). Hence we see that binding changes the sum, but not the difference of the helicity densities². Hence, the only modification of the spin dependent densities at the input scale occurs due to swelling. These are then evolved to the scale of interest.

At the time of interaction, the second binding effect applies to struck partons with momentum fraction $x \leq x_0$, as in the unpolarised case. The mechanism for this depletion is independent of the helicity of the quark, and so this effect is identical in both the spin independent as well as spin dependent cases.

²It is possible that ρ , etc., mesons also participate in this interaction, leading to a change in the polarised sea densities, but this component is small and we neglect it.

4.2 The Structure Function, $g_1^A(x, Q^2)$

The spin dependent structure function, $g_1^A(x, Q^2)$ can now be computed by evolving the modified input spin dependent densities to the required value of Q^2 , and including the second binding effect. We display the equivalent neutron bound-nucleon structure functions at an arbitrary scale, $Q^2 > \mu^2$ (with $R = \sigma_L/\sigma_T = 0$) :

$$\begin{aligned} F_1^{n/A}(x, Q^2) &= \frac{1}{18} \left[u_v^A(x, Q^2) + 4 d_v^A(x, Q^2) + K'(A) S_A(x, Q^2) \right] , \\ g_1^{n/A}(x, Q^2) &= \frac{1}{18} \left[\tilde{u}_v^A(x, Q^2) + 4 \tilde{d}_v^A(x, Q^2) + K'(A) \tilde{S}_A(x, Q^2) \right] . \end{aligned} \quad (20)$$

$q^A(\tilde{q}^A)(x, \mu^2)$ incorporates the effect of swelling on every input parton density, $q^N(\tilde{q}^N)(x, \mu^2)$, as well as that of binding for the unpolarised densities, and the corresponding Q^2 -dependent quantities that appear here are these input densities, evolved suitably to the required scale. $K'(A)$ incorporates the second binding effect at Q^2 , as discussed above. The experimentally measured asymmetry, and quantity of interest, are the ratios, at the scale Q^2 , for the neutron bound in the helium nucleus and for a free neutron:

$$\mathcal{A}^{\text{meas}} = \frac{g_1^{n/\text{He}}}{F_1^{n/\text{He}}} , \quad \mathcal{A}^{\text{free}} = \frac{g_1^n}{F_1^n} , \quad (21)$$

and can thus be computed. We use the free and bound nucleon *unpolarised* structure functions as computed in the previous section. Note that the input spin dependent densities (which are taken from [19]) were actually fitted to both the free proton as well as deuteron and ^3He spin dependent data; however, we use them here as the free nucleon parametrisations (which is permissible especially in view of the large error bars on presently available data). Furthermore, the smearing effect of Fermi motion (at large x) is neglected as in the unpolarised case. Hence our results are not valid at large x .

In fig. 5 we give the results of our computations for the measured (bound nucleon) and required (free nucleon) spin dependent structure function, g_1^n for typical values of Q^2 , $Q^2 = 1, 4 \text{ GeV}^2$. We see that the deviations of the bound neutron structure function can be as large as 10–15% at small x and about 6% at intermediate x values. The data points plotted on this graph correspond to the values extracted at $Q^2 = 4 \text{ GeV}^2$ from a measurement of the asymmetry by the E142 Collaboration [27] (with $R = 0$) and indicate the size of the error bars in currently available data.

In fig. 6, we plot the asymmetries at $Q^2 = 4 \text{ GeV}^2$. The data points here correspond exactly to the E142 data and therefore go over a range of Q^2 with a mean of about 2 GeV^2 ;

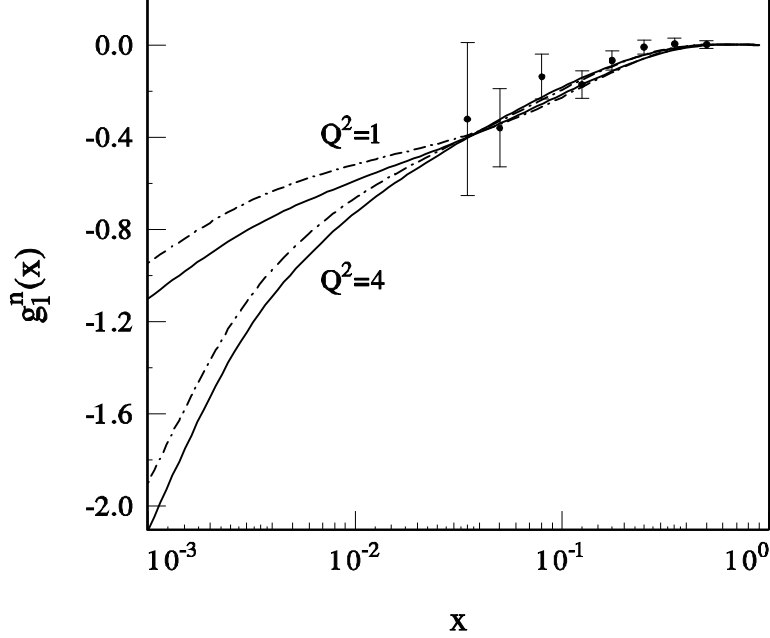


Figure 5: The free and bound nucleon spin dependent structure function for $Q^2 = 1, 4 \text{ GeV}^2$ as a function of x are shown as solid and dashed lines respectively. The structure function data are extracted at $Q^2 = 4 \text{ GeV}^2$ from the asymmetries measured by the E142 collaboration.

however, the asymmetry is not very sensitive to Q^2 in the x range of the available data. Notice that in this case, nuclear effects cause not more than 5% deviation in the asymmetry at both small and intermediate values of x . The deviation is slightly larger at larger x , $x > 0.4$, but this is due to the fact that the neutron spin dependent structure function changes sign near this value, and hence this deviation cannot be considered to be significant.

The asymmetry can also be expressed in terms of the EMC ratios,

$$R^A = \frac{F_2^{n/A}}{F_2^n} ; \quad \tilde{R}^A = \frac{g_1^{n/A}}{g_1^n} , \quad (22)$$

for the spin independent and spin dependent structure function ratios respectively. We have, for the helium case,

$$\mathcal{A}^{\text{meas}} = \frac{g_1^{n/\text{He}}}{F_1^{n/\text{He}}} = \frac{\tilde{R}^A}{R^A} \cdot \mathcal{A}^{\text{free}} . \quad (23)$$

Our results therefore indicate that

$$\mathcal{A}^{\text{meas}} \simeq \mathcal{A}^{\text{free}} ,$$

or, equivalently, that

$$\tilde{R}^A \simeq R^A , \quad (24)$$

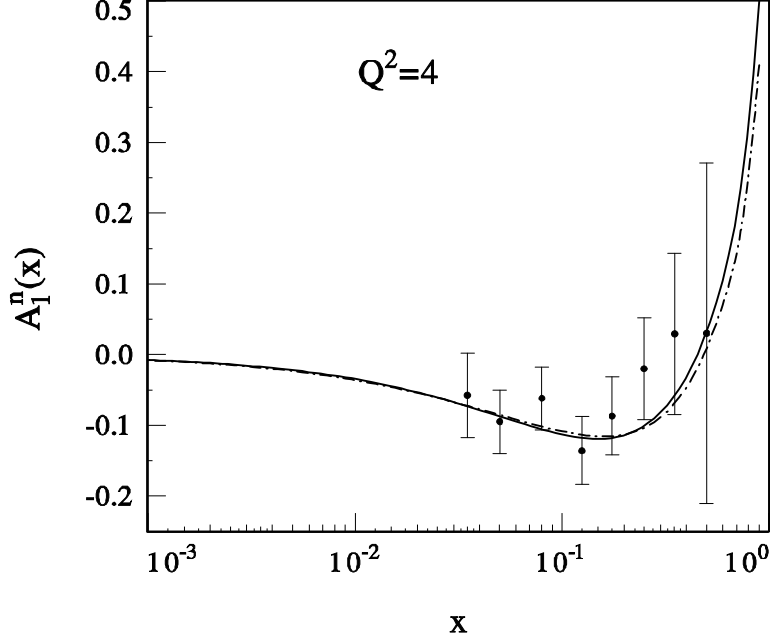


Figure 6: The bound and free nucleon asymmetries for $Q^2 = 4 \text{ GeV}^2$ as a function of x are shown as solid and dashed lines respectively. The data are from the E142 collaboration.

over most of the observed x region. Another (more experimentally relevant) way of stating this is to examine the difference between the following spin dependent structure functions:

$$\begin{aligned} g_1^n &= \mathcal{A}^{\text{free}} F_1^n ; \\ g_1' &= \mathcal{A}^{\text{meas}} F_1^n . \end{aligned} \quad (25)$$

The latter is actually what is extracted from polarised deep inelastic scattering data while the former is the theoretical quantity of interest. To a good approximation, however, these are numerically the same, due to (23) and (24). Finally, it may be remarked that, although $F_2^{n/A}$ is not known, the unpolarised bound-nucleon *isoscalar* structure functions are known; hence it *is* possible to extract the potentially interesting quantity, $g_1^A(x, Q^2)$, from future polarised experiments on isoscalar nuclear targets (HERMES, for instance, is a possibility) using,

$$g_1^A = \mathcal{A}^{\text{meas}} \cdot F_1^A .$$

It would then be possible to study the nuclear dependence of *polarised* structure functions, which would certainly shed a great deal of light on the nature of the EMC effect.

In short, we see that nuclear effects in the polarised helium data, though significant, equally affect both the spin dependent as well as the spin independent structure functions

in such a way that the measured asymmetries are to a great extent independent of them. Since it is the asymmetry rather than the structure function which is measured in a polarised experiment, much smaller errors on data are required before these small deviations due to nuclear effects become observable in such experiments. On the other hand, as already stated, this seems to make possible clean and unambiguous extraction of the relevant *free nucleon* structure functions from a measurement of double spin asymmetries with such light nuclear targets.

5 The Valence Densities

So far we have made a comparison of the structure functions with the data, and found good agreement. Our model parametrises the effects of nuclear interactions in a simple manner to obtain the bound nucleon densities in a nucleus; however, there are as many as three different effects that determine the densities, and the corresponding structure functions. The valence densities constitute the cleanest sector, as they are influenced by exactly one nuclear effect, viz., swelling. They thus form a good test of the *detailed* correctness of our model in terms of its individual component parts. The valence sector is already tested by current data in the large x region, where the structure function is dominated by the valence densities. We now look at the valence behaviour in the entire x region. It is possible to study this in either charged current deep inelastic processes (by studying the nuclear behaviour of the non-singlet structure function, $F_3(x, Q^2)$) [31], or, what is perhaps experimentally more feasible, in semi inclusive hadroproduction in the neutral current process [32, 33]. The quantity of interest here is the ratio of the difference in rates of production of the positive and negative charged hadron in a nucleus and a free nucleon respectively. It is defined to be

$$R^{\text{val},A} = \frac{[\mathcal{N}^{h^+} - \mathcal{N}^{h^-}]^A}{[\mathcal{N}^{h^+} - \mathcal{N}^{h^-}]^N},$$

where \mathcal{N}^{h^+} (\mathcal{N}^{h^-}) is the production rate (arbitrarily differential with respect to various kinematical variables) of a hadron (its charge conjugate). Here N refers to an “isoscalar nucleon” and h refers to pions, kaons, or protons, for example. The advantage of defining such a ratio is that the unknown fragmentation functions cancel out in the ratio, within the approximation that the fragmentation of the final state hadron is independent of the initial

deep inelastic scattering process (factorisation) and depends only on the momentum fraction of the parton which fragments into the hadron.

More specifically, the ratio in pion or kaon production from an isoscalar nucleus, A , is

$$R^{\text{val},A} = \frac{(u_V^A + d_V^A)}{(u_V^N + d_V^N)}. \quad (26)$$

Hence such a measurement yields information on just the valence sector (the isoscalar combination) alone, and over the entire x region. We therefore plot this ratio for two different nuclei, Carbon, and Calcium, as a function of (x, Q^2) in fig. 7. The large x ratio (which is essentially the same as the ratio of the corresponding structure functions) is already in agreement with data; the smaller x ratio exhibits shadowing, which decreases with increasing Q^2 , but is still substantial at $Q^2 = 15 \text{ GeV}^2$.

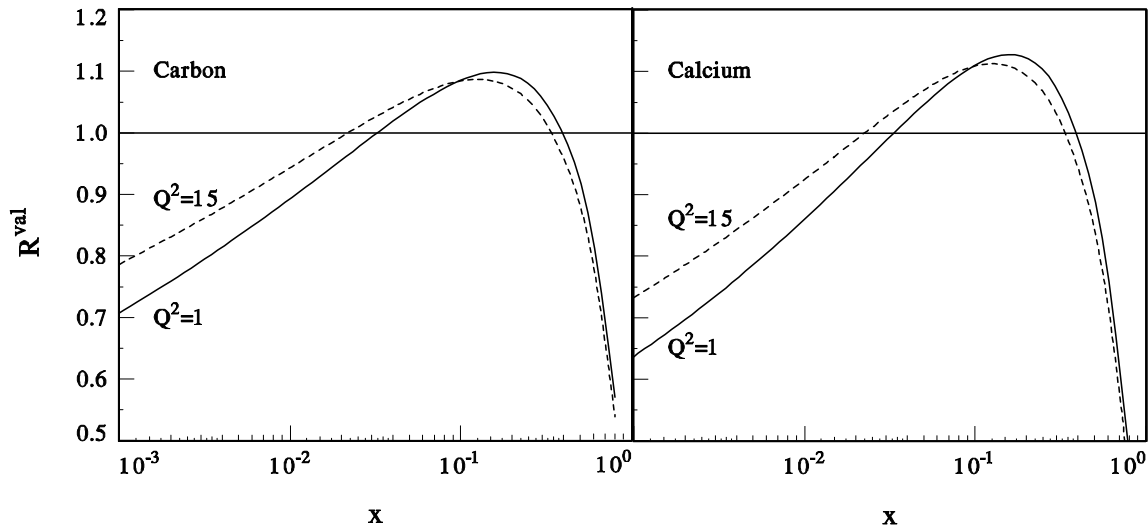


Figure 7: The valence ratios, $R^{\text{val},A}$, for Carbon and Calcium at two different values of Q^2 , plotted as a function of x .

The NMC data at low x correspond to rather small values of Q^2 ; hence, a study of semi-inclusive hadroproduction in such fixed target experiments should show large shadowing in the valence sector. This is in direct contrast to rescaling models which exhibit depletion at medium x (in the traditional EMC effect region) and antishadowing at smaller x values in the valence sector [31]. This is because, as we have discussed earlier, binding causes a depletion of the *valence* densities in such models at larger x , forcing a corresponding antishadowing at

smaller x (in accordance with momentum conservation). In contrast, binding depletes the *sea* densities in our model, while the effect of swelling causes depletion of the densities at both small and large x values. We remark that the aligned jet model also predicts a shadowing [33] of the valence ratio in (26), which is similar to the one we obtain; however, here the depletion is due to multiple scatterings. Hence, a measurement of the valence bound-nucleon densities in the small x region will certainly discriminate between some of the models that are currently available.

It is also possible to make a similar measurement in the *spin dependent* sector; it turns out that the corresponding ratio, for instance, for helium again, is not very different from the unpolarised result. This is because the valence asymmetry, which is the analogue of (23) for the valence quarks alone, is again largely insensitive to A , just as in the case of the asymmetry with respect to the total structure functions. Hence, shadowing at small x of the valence structure functions is predicted for both the polarised and unpolarised measurements.

6 Conclusion

We have constructed a model to compute nuclear modifications of nucleon structure functions and have used it to compute spin independent as well as spin dependent bound nucleon structure functions. The model uses both swelling and binding effects and is in good agreement with existing data. The swelling effect causes a modification of the bound-nucleon structure function itself, rather than causing just a scale change, as in traditional models of the nuclear EMC effect, and effectively gives rise to the observed intermediate- x “anti-shadowing”. The modified parton distributions are completely specified in terms of the free distributions, using fairly general conditions such as energy–momentum constraints and the Uncertainty principle, and using just one free parameter for the entire set of nuclei with different mass-numbers, A . Binding effects cause a depletion of the sea (or mesonic) densities in a bound nucleon. The extent of depletion is completely determined in terms of fundamental nuclear parameters. Both swelling and binding thus determine the input bound–nucleon densities, which are then dynamically evolved to the scale of interest. Finally, a second binding effect, caused by parton–nucleon overlap at the time of interaction, is introduced. This causes a further depletion of the small- x densities; the binding effects together account for the observed “shadowing” of the small- x structure functions. Hence our model satisfactorily

explains the observed EMC effect with remarkably few input parameters. In the case of polarised scattering, the model predicts that the measured asymmetries may not be sensitive to the nuclear modifications. Finally, a measurement of semi-inclusive hadroproduction in deep inelastic scattering experiments with nuclear targets, or the more ambitious one with polarised nuclear targets, will give information on nuclear modifications of valence densities in a different kinematical region as that probed by the corresponding inclusive process.

In short, we have a comprehensive model of nuclear structure functions that uses well-known parametrisations of the free nucleon parton densities and modifies them due to nuclear effects in a deterministic manner. The nuclear input is kept simple, with few free parameters, and the agreement of the model with data is satisfactory. Just as the general properties of the nuclear force originated from the binding effect of nuclei in the history of nuclear physics, we expect that a new understanding of binding effects in the EMC effect will bring to light the nature of the nuclear force at the level of quarks and gluons.

Acknowledgements: We thank M. Glück and E. Reya for extensive discussions and continuous encouragement, as well as for a critical reading of the manuscript. We thank M. Stratmann for providing the relevant FORTRAN programs. One of us (W. Z) acknowledges the support of the DAAD–K. C. Wong Fellowships and the National Natural Science Foundation of China and the hospitality of the University of Dortmund where part of this work was done.

References

- [1] J. J. Aubert *et al.*, The EMC, Phys. Lett. B123 (1982) 275.
- [2] For a recent review, see M. Arneodo, Phys. Rep. 240 (1994) 301. Also see references in the earlier reviews of [3] and [4] below.
- [3] L.L. Frankfurt and M.I. Strikman, Phys. Rep. 160 (1988) 235.
- [4] R.G. Roberts, *The structure of the proton*, Cambridge University Press, Cambridge, 1990, Chapter 8.
- [5] P. Amaudruz *et al.*, The EMC, Z. Phys. C53 (1992) 73.
- [6] P. Amaudruz *et al.*, The NMC, Nucl. Phys. B441 (1995) 3.

- [7] M. Arneodo *et al.*, The NMC, Nucl. Phys. B441 (1995) 12.
- [8] I. Abt *et al.*, The H1 Collaboration, Nucl. Phys. B107 (1993) 515; M. Derrick *et al.*, The ZEUS Collaboration, Phys. Lett. B316 (1993) 412.
- [9] P. Amaudruz *et al.*, The NMC, Phys. Rev. Lett. 66 (1991) 2712; Phys. Lett. B295 (1992) 159.
- [10] M. Glück, E. Reya, and A. Vogt, Z. Phys. C48 (1990) 471; Z. Phys. C67 (1995) 433.
- [11] V.N. Gribov and L.N. Lipatov, Sov. J. Nucl. Phys. 15 (1972) 438; *ibid*, 675; Yu.L. Dokshitzer, Sov. Phys. JETP 46 (1977) 641; G. Altarelli and G. Parisi, Nucl. Phys. B 126 (1977) 298.
- [12] R. L. Jaffe, Phys. Rev. Lett. 50 (1983) 228.
- [13] F. E. Close, R. G. Roberts, and G. G. Ross, Phys. Lett. B129 (1983) 346.
- [14] J. Ashman *et al.*, EMC, Nucl. Phys. B.238 (1989) 1; D. Adams *et al.*, SMC, Phys. Lett. B329 (1994) 399; Erratum B339 (1994) 332; K. Abe *et al.*, SLAC-E143, Phys. Rev. Lett. 74 (1995) 346, and preprints SLAC-PUB-94-6508 and SLAC-PUB-95-6734.
- [15] D. Indumathi, University of Dortmund Preprint DO-95/21, 1995, to appear in Phys. Lett. B.
- [16] A.D. Martin, R.G. Roberts, and W.J. Stirling, Phys. Rev. D50 (1994) 6743.
- [17] J. Botts *et al.*, The CTEQ collaboration, Phys. Lett. B304 (1993) 159.
- [18] J. D. Sullivan, Phys. Rev. D5 (1972) 1732.
- [19] M. Glück, E. Reya, and W. Vogelsang, Phys. Lett. B359 (1995) 201.
- [20] R.L. Jaffe, F. E. Close, R. G. Roberts, and G. G. Ross, Phys. Lett. B134 (1984) 449, Phys. Rev. D31 (1985) 1004.
- [21] W. Zhu and J. G. Shen, Phys. Lett. B219 (1989) 107; W. Zhu and L. Qian, Phys. Rev. C45 (1992) 1397.

- [22] M. Ericson and A. W. Thomas, Phys. Lett. B128 (1983) 112; C. H. Llewellyn Smith, Phys. Lett. B128 (1983) 107; S.A. Akulinichev, S.A. Kulagin, and G.M. Vagradov, Phys. Lett. B158 (1985) 485.
- [23] D.M. Alde, *et al.*, The E772 Collaboration, Phys. Rev. Lett. 64 (1990) 2479.
- [24] C. F. von Weizsäcker, Z. Phys. 96 (1935) 431; H. A. Bethe and R. F. Bacher, Rev. Mod. Phys. 8 (1936) 82.
- [25] The radii and densities, (R_A fm, ρ fm $^{-3}$), of the various nuclei, as quoted in [5], are (2.6, 0.04) for ${}^6\text{Li}$, (2.5, 0.09) for ${}^{12}\text{C}$, and (3.5, 0.11) for ${}^{40}\text{Ca}$.
- [26] NMC preliminary data on Sn/C; A. Mücklich, PhD. Thesis, Ruprecht-Karls-Universität, Heidelberg, 1995.
- [27] W. Melnitchouk, G. Piller, and A.W. Thomas, Phys. Lett. B346 (1995) 165; L.D. Kaptari *et al.*, Phys. Lett. B321 (1994) 271; H. Khan and P. Hoodbhoy, Phys. Lett. B298 (1993) 181; M.V. Tokarev, Phys. Lett. B318 (1993) 559; B. Badelek and J. Kwiecinski, Nucl. Phys. B370 (1992) 278; L.L. Frankfurt and M.I. Strikman, Nucl. Phys. B405 (1983) 557.
- [28] R.M. Woloshyn, Nucl. Phys. A496 (1989) 749; C. Ciofi degli Atti, E. Pace, G. Salme, Phys. Rev. C46 (1992) R1591.
- [29] C. Ciofi degli Atti, S. Scopetta, E. Pace, G. Salme, Phys. Rev. C48 (1993) R968.
- [30] L.L. Frankfurt, V. Guzey, and M.I. Strikman, Tel Aviv University, Israel, preprint 1996, hep-ph9602301.
- [31] R. Kobayashi, S. Kumano, and M. Miyama, Phys. Lett. B354 (1995) 465.
- [32] D. Indumathi, and M.V.N. Murthy, *Nuclear effects on parton densities in deep inelastic lepton hadron scattering*, Extended Abstract, DAE Symposium on Nuclear Physics, Aligarh, India, 1989.
- [33] L.L. Frankfurt, M.I. Strikman, S. Liuti, Phys. Rev. Lett. 65 (1990) 1725.